

1
2 Transcriptional regulation of ACSL1 by CHREBP and NF-kappa B in macrophages during
3 hyperglycemia and inflammation

4
5
6
7
8 Prashanth Thevkar-Nagesh^{1,2}, Shruti Rawal², Tarik Zahr², Edward A. Fisher^{2*} and Michael J.
9 Garabedian^{1*}

10
11 ¹Department of Microbiology, New York University School of Medicine, New York, NY 10016,
12 USA.

13 ²Department of Medicine, New York University School of Medicine, New York, NY 10016, USA.

14
15 **Author Emails:**

16 Prashanth.ThevkarNagesh@nyulangone.org
17 srawal@bidmc.harvard.edu
18 Tarik.Zahr@nyulangone.org
19 Edward.Fisher@nyulangone.org
20 Michael.Garabedian@nyulangone.org

21
22 **Author contributions:**

23 Prashanth Thevkar-Nagesh; was involved with the investigation and analysis of the data, as well
24 as writing the original draft preparation of the manuscript; Shruti Rawal and Tarik Zahr were
25 involved in the investigation; Edward A. Fisher and Michael J. Garabedian were involved with
26 conceptualization, funding acquisition, project administration, supervision, writing the original
27 draft as well as its review and editing the final version of the manuscript.

28
29 ***Corresponding authors**

30
31 **Acknowledgements:** We thank Drs. Claudia Han and Christopher Glass (UCSD) for providing
32 the CHREBP knock out macrophages. We also thank Hussam Alkaissi (NYU) for help with the
33 ACSL1 membrane localization experiment. This work was supported by an NIH grant
34 (P01HL131481) to E.A.F and M.J.G.

35
36 **Key words:** Acyl-CoA synthetase 1 (ACSL1); transcription; CHREBP; NF-kappa B;
37 hyperglycemia; diabetes; inflammation; macrophage

38
39 **Running title:** Mechanism of Acsl1 transcriptional regulation

40

41 **ABSTRACT**

42 Acyl-CoA synthetase 1 (ACSL1) is an enzyme that converts fatty acids to acyl-CoA-
43 derivatives for use in both lipid catabolism and lipid synthesis, including of arachidonic acid
44 mediators that promote inflammation. ACSL1 has also been linked to the pro-atherosclerotic
45 effects of diabetes in mice. ACSL1 expression has been reported to be upregulated in
46 monocytes and macrophages by hyperglycemia, as well as enhanced by inflammatory stimuli,
47 yet surprisingly little is known about the mechanisms underlying its transcriptional regulation.
48 Here we show that increased *Acs1* mRNA expression in mouse macrophages by
49 hyperglycemia is via transcription initiation such that nascent ACSL1 RNA and *Acs1* promoter
50 activity are increased. We further demonstrate that the hyperglycemic-dependent induction of
51 *Acs1* mRNA is governed by the glucose-sensing transcription factor, Carbohydrate Response
52 Element Binding Protein (CHREBP), since the hyperglycemic upregulation of *Acs1* mRNA is
53 lost in mouse bone marrow derived macrophages (BMDMs) from *Chrebp* knock out mice. In
54 addition, we show that LPS treatment of mouse BMDMs increased *Acs1* mRNA, and this is
55 attenuated by an NF-kappa B inhibitor that blocks p65 subunit binding to DNA. We further show
56 that LPS treatment increased ACSL1 protein abundance and stimulated ACSL1 protein
57 localization to membranes where it likely exerts its activity. Using an ACSL1 reporter gene
58 containing the promoter and 1.6 Kb of upstream regulatory region, which contain multiple
59 predicted CHREBP and NF-kappa B (RELA) binding sites conserved between the human and
60 mouse ACSL1 gene, we found a synergistic increase of ACSL1 promoter activity when
61 CHREBP and RELA were co-expressed. Thus, we have identified pathways controlling the
62 expression of ACSL1 by hyperglycemia and inflammation through CHREBP and NF-kappa B.

63

64 INTRODUCTION

65

66 Atherosclerosis is a chronic inflammatory disease characterized by infiltration and
67 deposition of lipid laden macrophages, termed “foam cells”, in the arterial wall [1]. Circulating
68 monocytes are recruited to the plaque by inflammatory signals, and become activated
69 macrophages and proinflammatory, further contributing to the plaque development.

70 There are several factors that drive the inflammatory response of macrophages,
71 including the enzyme ACSL1, which converts long-chain fatty acids into acyl-CoA derivatives [2,
72 3]. When arachidonic acid (C20:4) is taken up by macrophages it is converted by ACSL1 to
73 arachidonoyl-CoA (20:4-CoA), which in turn is incorporated into phospholipids. This 20:4-CoA
74 moiety can be liberated from the phospholipids by phospholipase A2 (PLA2) and made
75 available for prostanoid production, and activation of prostaglandin-endoperoxide synthase
76 (PTGS; *aka* COX2) to enhance inflammation [3, 4].

77 ACSL1 has also emerged as a mediator of the enhanced atherosclerosis associated
78 with diabetes [3]. Diabetes increases the risk of cardiovascular disease by accelerating the
79 progression of atherosclerosis [5]. The expression of ACSL1 mRNA has been shown to be
80 increased in monocytes from human diabetic patients and mouse models of type-1 diabetes [4].
81 Moreover, this increased expression was also observed when macrophages were cultured
82 under diabetes-relevant high glucose (25mM) compared to normal glucose (5.5mM), suggesting
83 that the effect of hyperglycemia on ACSL1 expression is cell autonomous. Importantly, the
84 accelerated progression of atherosclerosis under diabetes was prevented in mice lacking *Acs1*
85 in monocytes and macrophages [4]. Thus, ACSL1 is a key regulator of the pro-atherosclerotic
86 effects of diabetes. Consistent with ACSL1 links to cardiovascular and metabolic disease in
87 humans, analysis of genome wide association studies found intronic SNPs in ACSL1 associated
88 with atherosclerosis and type-2 diabetes [6].

89 In addition to hyperglycemia, ACSL1 expression in macrophages is induced by
90 lipopolysaccharide (LPS) and gram negative bacteria (*E. Coli*) [7]. Moreover, inflammatory M1
91 macrophages showed not only an increased in the abundance of ACSL1 protein, consistent with
92 the increased mRNA, but greater ACSL1 protein localization to the plasma membrane relative
93 to non-activated (M0) macrophages, suggesting that membrane location of ACSL1 is part of its
94 proinflammatory response by aligning ACSL1's enzymatic activity to the site of its substrates [2].

95 Despite the increased expression of ACSL1 in macrophages by hyperglycemic and
96 inflammatory stimuli, little is known about the mechanisms mediating the transcriptional
97 regulation of ACSL1, including the transcription factors controlling ACSL1 expression. Here we
98 report the analysis of the mechanisms and transcription factors controlling ACSL1 expression.
99 We find that transcriptional regulation of ACSL1 under hyperglycemia and inflammatory stimuli
100 involve, respectively, CHREBP and NF-kappa B-mediated activation of the ACSL1 promoter.

101

102 **MATERIALS AND METHODS**

103 **Cell culture**

104 Human embryonic kidney (HEK) 293 cells (ATCC) were cultured in Dulbecco's modified Eagle's
105 medium (DMEM, Corning) containing 10% fetal bovine serum (FBS) and 1% PenStrep (100
106 U/mL Penicillium and 100ug/mL Streptomycin) in either 4.5 g/L D-glucose or 1 g/L D-glucose +
107 3.5 g/L L-glucose (Sigma) to serve as an osmotic control. Cells were tested for mycoplasma and
108 were tested negative. Cells were cultured with 5% CO₂ at 37°C.

109 **Animals**

110 Wild type mice (C57B16J) were obtained from Jackson labs. Tibias and femurs from *Mlxipl*
111 deficient mice (*Chrebp*^{-/-}) were kindly provided by Dr. Claudia Han from the Glass lab at UCSD.
112 The animals were cared for in accordance with the National Institutes of Health guidelines and
113 the NYU and UCSD Institutional Animal Care and Use Committee. Mice were euthanized by

114 CO₂ followed by cervical dislocation in accordance with approved guidelines for the euthanasia
115 of animals.

116 **Bone marrow derived macrophages (BMDMs)**

117 BMDMs were isolated from the tibia and femur of 6–12-week-old male C57BL6J mice. Isolated
118 bone marrow cells were treated with red blood cell lysis buffer (Sigma) and re-suspended in
119 differentiation medium (DMEM with 1 g/L D-glucose + 3.5 g/L L-glucose or 4.5 g/L D-glucose
120 and L-glutamine, supplemented with 20% FBS and 10 ng/μL macrophage colony-stimulating
121 factor (M-CSF) (PeproTech, Inc., Rocky Hill, NJ). Cells were passed through a 70 μm filter to
122 clear any debris. Following this, cells were plated in 10cm non-tissue coated plates and allowed
123 to differentiate for 7 days to obtain un activated (M0) macrophages. At day 7, the cells were
124 washed in PBS, and re-plated with desired cell density in a 6-well dish and allowed to attach to
125 the plate. Cells were treated with LPS (50ng/ml) for the indicated times, and RNA or protein was
126 isolated. For some experiments, NF-kappa B inhibitor, CAPE (5μM) was pretreated for 4 hours
127 before LPS treatment.

128 **Promoter motif prediction**

129 Eukaryotic Promoter Database was used for predicting the putative CHREBP (*Mlx1pl*) and p65
130 (RELA) sites on the upstream ACSL1 promoter using the mouse and human database [8].

131 **Luciferase assay**

132 HEK 293 cells (24 well format) were transfected with Lipofectamine 3000 (Invitrogen) following
133 manufacturers protocol. Cells were transfected with 250ng of vector only or ACSL1-GL or
134 CHREBP+ ACSL1-GL or p65 (RELA) + ACSL1-GL constructs. For co-transfection experiments,
135 p65 (RELA) (250ng) and were CHREBP (250ng) were co-expressed with ACSL1-GL and the
136 vector only was adjusted to 750ng. At 48 hour post transfection, media was collected from the
137 respective cells and luciferase assay was performed following manufacturer's protocol with GL-
138 S buffer. Luciferase activity was measured using the LMax microplate reader luminometer with
139 an integration time of 3 sec. The ACSL1-Gaussian luciferase (GL) reporter construct and control

140 Gaussian luciferase vectors were obtained from Genecopeia (Product ID: MPRM39476).
141 pcDNA3 Flag-RelA was purchased from Addgene (plasmid #20012) and deposited by Stephen
142 Smale [9]. The ChREBP expression vector was purchased from Addgene (plasmid #39235)
143 and deposited by Isabelle Leclerc [10].

144 **RNA isolation, cDNA synthesis and qPCR**

145 Total RNA was isolated using RNeasy Mini Kit (Qiagen). On-column DNase digestion step was
146 performed during the isolation process. cDNA was synthesized from 500ng of RNA using
147 Thermo Scientific™ Verso cDNA Synthesis Kit (AB1453B) following the manufacturer's
148 instructions. Quantitative real-time PCR was performed on the QuantStudio 6 Flex (Applied
149 Biosystems) using SYBR Green Fast Master Mix (Applied Biosystems). 5ng of cDNA and
150 100nM primers were used for performing the qPCR reaction. Gene expression was calculated
151 using the relative quantification ($2^{-\Delta\Delta CT}$ method) or by absolute quantification using standard
152 curve.

153 **Primers**

154 ACSL1 mRNA

155 F 5'-GCGGAGGAGAATTCTGCATAGAGAA-3';

156 R 5'-ATATCAGCACATCATCTGTGGAAG-3'

157 Cyclophilin A1 mRNA

158 F: 5'-GGCCGATGACGAGCCC-3'

159 R: 5'-TGTCTTTGGAACCTTTGTCTGCAA-3'

160 ACSL1 hnRNA

161 F: 5'-TCACTCCTTATCACCTCTTC-3'

162 R: 5'-CTCCAGAGCTTTGAGGCTGATG -3'

163 **Immunoblotting**

164 Cells were lysed in lysis buffer (50 mM Tris-HCl [pH 7.4], 150 mM NaCl, 0.5% sodium dodecyl
165 sulfate [SDS], 0.5% sodium deoxycholate, 1% Triton X-100, and 1× protease inhibitor cocktail

166 [Roche]). The total amount of protein was quantitated by using Pierce™ Rapid Gold BCA
167 Protein Assay Kit (Thermo Scientific). Equal amounts of proteins were resolved on 10 or 15%
168 Tris-glycine SDS-PAGE under reducing conditions and transferred onto Immobilon-P
169 Membrane, PVDF, 0.45 µm (Millipore). Membranes were probed with rabbit anti-ACSL1 (#9189,
170 1:1,000; Cell Signaling), rabbit anti-CHREBP Antibody (# NB400-135, 1:500; Novus
171 Biologicals), rabbit anti-histone H3 (1:1,000; Cell Signaling), rabbit anti-actin (1:5,000; Abcam),
172 rabbit-anti Sodium Potassium ATPase antibody (1:5,000; ab76020, Abcam) or mouse anti-
173 tubulin Mouse Monoclonal Antibody (HRP-66031, 1:5000, Proteintech), followed by horseradish
174 peroxidase-conjugated anti-mouse, or anti-rabbit IgG antibody (1:5,000; Life Technologies).
175 Protein bands were visualized by using a Clarity Western ECL Substrate (BioRad), and images
176 were acquired on an Odyssey Fc imaging system (Li-Cor).

177 **Immunofluorescence**

178 Cells were fixed in 4% methanol-free paraformaldehyde (Fisher Scientific) and permeabilized
179 with 0.2% Triton X-100. 5% mouse or rabbit serum was used for blocking. Cells were stained
180 with rabbit anti-CHREBP antibody (# NB400-135, 1:100; Novus Biologicals), followed by Alexa
181 488-conjugated goat anti-rabbit IgG secondary antibody (1:400; Invitrogen) for 1 hour at room
182 temperature. Finally, cells were stained with the DNA-binding dye Hoechst (5 µg/ml;
183 Invitrogen), and coverslips were mounted in mounting medium (Sigma-Aldrich). Fluorescent
184 images were acquired by sequential scanning on a Leica SP5 Confocal Microscope confocal
185 laser scanning microscope. Acquired images were analyzed in ImageJ.

186 **Statistical analysis**

187 All statistical analyses were performed using Prism 6 (GraphPad). P values were calculated by
188 using unpaired t tests for pairwise data comparisons, one-way analysis of variance (ANOVA), or
189 two-way ANOVA for multiple comparisons. A P value of ≤ 0.05 was considered significant.

190

191

192 **RESULTS**

193 ***Acs11* expression is transcriptionally upregulated in macrophages under hyperglycemia**

194 It has been reported that the expression of *Acs11* is upregulated in diabetic monocytes
195 and macrophages *in vitro*, *in vivo*, and in clinical samples [4, 6, 11] However, the mechanism
196 whereby *Acs11* is upregulated by hyperglycemia is not understood. For instance, is the increase
197 in *Acs11* mRNA by high glucose a result of an increase in the transcriptional initiation of the
198 gene? To interrogate the regulation of *Acs11*, we differentiated primary mouse bone marrow
199 derived macrophages (BMDMs) under normal glucose (NG; 5.5 mM glucose) and high glucose
200 (HG; 25mM glucose) conditions. We found that *Acs11* mRNA and protein were upregulated
201 under HG compared to NG (Fig. 1A and B). To identify if this increase reflected enhanced
202 transcription, we measured the levels of heteronuclear, or nascent RNA as a surrogate for
203 newly synthesized *Acs11* transcripts indicative of transcriptional initiation [12]. We found that the
204 increase in steady state *Acs11* mRNA was associated with a corresponding increase in the
205 nascent RNA levels under HG as compared to NG conditions (Fig. 1C). This indicates that
206 hyperglycemia induces the transcription of *Acs11* gene in mouse BMDMs.

207 To further extend these observations, we measured *Acs11* promoter activity by
208 performing luciferase assays in HEK293 cells transfected with an *Acs11* construct containing the
209 *Acs11* promoter, and ~1.5 Kb of upstream regulatory DNA fused to the Gaussia luciferase gene
210 (pACSL1-GLuc) under NG and HG conditions. Cells cultured in NG or HG were transfected
211 with pACSL1-GLuc construct or with a control empty luciferase vector without the ACSL1
212 sequences for 48 hours before luciferase was measured. Luciferase activity was higher in cells
213 cultured in HG as compared to NG containing the pACSL1-GLuc construct (Fig. 1D). The
214 empty vector showed no difference in activity between high and low glucose (not shown). This
215 is consistent with the effect of hyperglycemia on *Acs11* mRNA expression controlled at the level
216 of transcriptional initiation of the *Acs11* promoter.

217

218 **CHREBP regulates *Acs11* transcription under hyperglycemia**

219 CHREBP is a glucose responsive transcription factor that regulates metabolic genes,
220 including those involved in lipolysis and glycolysis [13-15]. An increase in intracellular glucose
221 levels relieves inhibition of CHREBP and promotes CHREBP translocation from the cytoplasm
222 into the nucleus, where it drives the expression of glucose responsive genes [16]. Elevated
223 glucose levels in diabetes is has been shown to increase CHREBP transcriptional activity in
224 liver and adipose tissue [17]. In addition, a ChIP-seq study for CHREBP from white adipose
225 tissue from the fasted to fed state showed CHREBP occupies multiple sites upstream of the
226 *Acs11* transcription start site [18], suggesting that a *Acs11* is a potential target of CHREBP.
227 Because the induction of *Acs11* by hyperglycemic is at the transcriptional level, and that
228 CHREBP occupies an upstream regulatory region of *Acs11* in adipose tissue, we hypothesized
229 that the induction of *Acs11* by hyperglycemia in macrophages is through CHREBP. To
230 investigate this we used both gain and loss of function approaches. Prior to embarking on these
231 experiments, we first determined the localization of CHREBP in BMDMs cultured under NG and
232 HG conditions. We observed an increase in CHREBP nuclear localization under HG compared
233 to NG conditions by cell fraction and immunofluorescence (S1_fig.pdf). This is consistent with
234 CHREBP being a potential transcriptional activator of *Acs11* under HG conditions.

235 Next, we used a gain of function approach to determine whether overexpression of
236 CHREBP regulates *Acs11* promoter activity in a cell based reporter assay. We co-transfected
237 HEK293 cells with the same pACSL1-GLuc reporter as in Figure 1D, along with a CHREBP
238 expression construct, or an empty expression vector, under NG and HG conditions. *Acs11*
239 promoter activity was higher in the cells expressing CHREBP in both NG and HG conditions
240 (Fig 2A). The basal promoter activity in cells with vector only was also higher in the HG
241 condition as compared to NG, and the *Acs11* promoter activity was further increased in cells
242 cultured in HG and overexpressing CHREBP (Fig. 2A). This is consistent with CHREBP
243 inducing *Acs11* transcription in HG.

244 To further examine the impact of CHREBP on glucose-dependent *Acs1* transcriptional
245 activation we turned to a loss of function approach. We evaluated *Acs1* expression in the
246 absence of CHREBP under NG and HG conditions using macrophages from *Chrebp*^{-/-} mice [15].
247 BMDMs from wild type littermate and *Chrebp*^{-/-} mice were differentiated under NG and HG
248 conditions, and *Acs1* mRNA expression was measured. *Acs1* expression was reduced in
249 *Chrebp*^{-/-} cells in both NG and HG conditions, with a greater reduction in *Acs1* expression in HG
250 from *Chrebp*^{-/-} cells compared to wild type controls (Fig. 2B). This result indicates that CHREBP
251 is required both for basal and glucose-induced expression of *Acs1*.

252

253 **Lipopolysaccharide (LPS) stimulates *Acs1* expression under NG and HG**

254 Previous reports indicate that *Acs1* expression is induced by inflammatory mediators,
255 including LPS [7], and also is important in the TNF α -mediated inflammatory response in
256 monocytes and macrophages [19]. It has also been reported that diabetic subjects have higher
257 levels of *ACSL1* mRNA in circulating inflammatory monocytes [4]. Moreover, in a preclinical
258 mouse model, myeloid specific deletion of *Acs1* decreased the expression of proinflammatory
259 cytokines under diabetic condition [4]. While it is evident that several pathways are capable of
260 upregulating *Acs1* mRNA in macrophages [3], the specific transcription factors mediating the
261 induction of *Acs1* via inflammatory stimuli, and how inflammatory and hyperglycemic signals
262 intersect to promote *Acs1* expression is not understood.

263 To address the regulation of *Acs1* by inflammatory signals, we performed a time course
264 experiment to determine the kinetics of *Acs1* induction to LPS in macrophages. We found an
265 induction of *Acs1* in BMDMs between 3 and 6 hours post LPS treatment, with longer time
266 points resulting in higher levels of *Acs1* mRNA (S2_fig.pdf). Since a significant increase in
267 *Acs1* mRNA expression was observed at 24 hours, this timepoint was selected for subsequent
268 experiments.

269 Given our interest in diabetes and the induction of *Acs/1* mRNA by hyperglycemia, we
270 evaluated the impact of not only inflammation, but the combination of inflammation with
271 hyperglycemia to *Acs/1* expression in macrophages. The results indicate that LPS treatment of
272 macrophages (which results in M1 activated macrophages) in NG induced *Acs/1* expression
273 ~40 fold as compared to BMDMs not activated by LPS (M0 macrophages) (Fig. 3A).
274 Intriguingly, *Acs/1* expression upon LPS treatment in HG-induced cells increased ~80-fold
275 relative to BMDMs not activated by LPS in NG. We also observed an increase ACSL1 protein
276 abundance and localization to membranes upon LPS treatment (S3_fig.pdf) as has been
277 described by others [4]. This suggests that both inflammatory and hyperglycemic signals
278 contribute to the regulation of *Acs/1*.

279 We also compared the localization of CHREBP protein in unstimulated (M0) and LPS-
280 treated inflammatory (M1) macrophages under NG and HG conditions. M1 macrophages show
281 increased nuclear CHREBP both in NG and HG conditions, with a slight increase in nuclear
282 CHREBP under HG conditions (Fig. 3B). This suggests that CHREBP is contributing to the
283 transcriptional regulation of ACSL1 during inflammation especially under HG conditions.

284 Since LPS stimulates via Toll like receptors (TLRs) the activation of NF-kappa B [20, 21],
285 we examined whether the LPS-dependent induction of *Acs/1* was reduced by inhibition of NFkB
286 using caffeic acid phenethyl ester (CAPE), an inhibitor that blocks NF-kappa B binding to DNA
287 [22]. BMDMs cultured under HG conditions were either left unactivated (M0) or activated with
288 LPS (M1) in the absence and presence of CAPE. CAPE treatment reduced LPS-dependent
289 induction of *Acs/1* expression in macrophages (M1), while inhibiting NF-kappa B in the absence
290 of LPS treatment did not affect the expression of *Acs/1* in M0 macrophages (Fig. 3B). This
291 suggests that NF-kappa B activation contributes to *Acs/1* expression as a function of
292 inflammatory stimuli, although additional factors, including but not limited to CHREBP may also
293 participate in *Acs/1* transcription under inflammatory and hyperglycemic conditions.

294

295 **CHREBP and RELA synergistically activate *Acs1* promoter**

296 Given that both NF-kappa B and CHREBP appear to modulate *Acs1* expression, we
297 examined the 1.6 kb upstream regulatory region of the mouse and human *Acs1* genes for
298 putative ChoRE (binding site for CHREBP) and RELA (binding site for NF-kappa B) sites using
299 the Eukaryotic Promoter Database [8] that incorporates the Jaspar database to predict
300 transcription factor binding site [23]. Multiple CHREBP and RELA binding sites were identified
301 ($p < 0.01$) in close proximity to one another that were conserved between the mouse and human
302 genes (S4_fig.pdf). Such conservation is suggestive of the importance of the sites in
303 transcriptional regulation [24].

304 To test the functional significance of NF-kappa B and CHREBP in establishing *Acs1*
305 gene expression, we employed a cell based reporter assay using the pACSL1-GLuc reporter
306 gene containing the ~1.6 kB of upstream regulatory sequence. We transfected HEK293 cells
307 with pACSL1-GLuc, with expression vectors for CHREBP or RELA separately, or CHREBP and
308 RELA together, and measured the *Acs1* promoter activity. While there was a modest increase
309 in pACSL1-GLuc activity in cells transfected with CHREBP, there was no increase in reporter
310 activity with RELA alone (Fig. 4). Strikingly, co-expression of CHREBP and RELA showed a
311 synergistic increase *Acs1* promoter activity (Fig. 4). This suggests that CHREBP and NF-
312 kappa B act together to increase *Acs1* transcriptional activity.

313

314 **DISCUSSION**

315 ACSL1 is one of a family of enzymes that promotes the thioesterification of long-chain
316 fatty acids to form acyl-CoAs for use in synthetic or degradative pathways [2, 3]. In
317 metabolically active tissues the acyl-CoAs go toward mitochondrial β -oxidation. ACSL1 can
318 also specify phospholipid synthesis, and these can serve as a source of arachidonic acid-CoA
319 metabolites that support prostaglandin synthesis to fuel inflammation in diabetes that
320 exacerbates atherosclerosis [4]. Whereas *Acs1* mRNA expression is controlled by

321 inflammation and hyperglycemia, the mechanisms underlying the induction of *Acs1* mRNA by
322 these stimuli have remained enigmatic. In this study, we defined transcription factors controlling
323 *Acs1* gene expression in macrophages. We show that *Acs1* expression is regulated by
324 CHREBP in hyperglycemia and through NF-kappa B under inflammatory conditions. This is
325 consistent with recent reports showing increased ACSL1 mRNA in peripheral blood from septic
326 patients [25], and also elevation in blood of patients with acute myocardial infarction compared
327 to controls [11], which may reflect an inflammatory response from necrotic tissue as a result of
328 ischemia.

329 CHREBP appears to control *Acs1* mRNA expression in both NG and HG in M0
330 macrophages, suggesting even under NG there is some active CHREBP, which becomes
331 increased in HG to promote *Acs1* transcription. This suggests that CHREBP under
332 hyperglycemia is a key determinant in the increased expression of *Acs1* observed in monocytes
333 and macrophages from both humans and mice under conditions of diabetes. This is reflected in
334 the glucose-dependent induction of *Acs1* steady state mRNA and nascent RNA expression,
335 and the overexpression and deletion of CHREBP that increased and decreased, respectively,
336 *Acs1* transcriptional activity.

337 Acute inflammatory stimuli by LPS in macrophages promotes a robust induction of *Acs1*
338 mRNA. This can be largely suppressed by an NF-kappa B inhibitor. Although it appears that
339 induction of *Acs1* transcription by LPS predominates relative to the expression under
340 hyperglycemia, the inflammatory response of *Acs1* expression can be further enhanced in
341 hyperglycemic conditions, suggesting an interplay between pathways. Consistent with this is
342 the synergistic increase in *Acs1* promoter activity when both CHREBP and RELA were co-
343 expressed, suggesting the two factors cooperate to drive *Acs1* gene expression in settings of
344 inflammation and hyperglycemia. This is also in line with binding sites for both factors being
345 present in the upstream ACSL1 regulatory region and conserved between the mouse and
346 human genes. Such conservation is often sufficient to predict transcription factor occupancy

347 and activity at induced genes [24]. Indeed, CHREBP has been shown to occupy the *Acs/1*
348 upstream regulatory region in mouse adipose tissue [18], and analysis of the human ACSL1
349 gene from ENCODE shows RELA occupancy in the region upstream of the ACSL1 start site of
350 transcription in a variety of cells types. This is reinforced by the functional studies that indicate
351 both CHREBP and NF-kappa B enhance the expression of *Acs/1*.

352 Based on these findings, we propose that in macrophages under conditions of NG and
353 either no or low level inflammation the expression of *Acs/1* is low and driven by a small pool of
354 active, nuclear CHREBP (Fig. 5A). Expression of *Acs/1* is increased under conditions of HG by
355 virtue of an increase in the pool of nuclear CHREBP (Fig. 5B). We further posit that in
356 macrophages exposed to an acute inflammatory stimuli, such as by LPS, expression is of *Acs/1*
357 is increased by activation of NF-kappa B under both NG and HG, with even greater activation in
358 HG (Fig.5C). Whether NF-kappa B induction of *Acs/1* also requires CHREBP remains an open
359 question, but is suggested by the low activity of the *Acs/1* reporter with overexpressed RELA,
360 and that co-expression of both CHREBP and RELA synergistically activate the *Acs/1* reporter.
361 Thus, our studies have revealed the convergence of two important pathways on the regulation
362 of *Acs/1* in macrophages to align the production of acyl-CoA derivatives to the cellular
363 environment.

364

365 **FIGURE LEGENDS**

366 **Figure 1. ACSL1 expression is transcriptionally upregulated in macrophages under**

367 **hyperglycemic.** A) BMDMs were differentiated under normal glucose (NG) and high glucose

368 (HG) and *Acs/1* mRNA copy number was determined by quantitative real-time PCR (qPCR). B)

369 Western blot of total cell lysates from BMDMs cultured in NG and HG using antibodies against

370 ACSL1 and β -actin as a loading control. C) *Acs/1* nascent RNA expression was determined by

371 qPCR using primers spanning the intron-exon junction relative to cyclophilin A1 and shown as

372 fold change between NG and HG. D) pACSL1-GLuc reporter was transfected in HEK 293 cells

373 cultured under NG and HG conditions. Luciferase assay was performed 48 hours post
374 transfection, and presented a relative luciferase units (RLU). The data presented are means \pm
375 standard errors of the means of three independent experiments; the *P* value was calculated
376 using students *t* test. Levels of significance denoted as **p* < 0.05 and ***p* < 0.01.

377

378 **Figure 2. CHREBP contributes to transcriptional upregulation of ACSL1 under**

379 **hyperglycemia.** A) CHREP expression plasmid or vector only (VO) were co-transfected with
380 pACSL1-GLuc reporter in HEK 293 cells cultured under NG and HG conditions. Luciferase
381 assay was performed 48 hours post transfection and shown as relative luciferase units (RLU)..

382 B) Wild type or *Chrebp*^{-/-} BMDMs were differentiated under NG and high glucose HG conditions.
383 *Acs11* mRNA copy number was determined by quantitative real-time PCR (qPCR). The data
384 presented are means \pm standard errors of the means of three independent experiments; the *P*
385 value was calculated using one way ANOVA. Levels of significance: **p* < 0.05; ***p* < 0.01; and
386 ****p* < 0.001.

387

388 **Figure 3. LPS induction of *Acs11* expression is via NF-kappa B.** A) BMDMs were

389 differentiated under NG and HG conditions. Cells were treated with LPS (50ng/ml) for 24 hours.
390 Total RNA was isolated, cDNA was synthesized and *Acs11* mRNA was determined by qPCR
391 relative to cyclophilin A1 mRNA and shown as fold change with M0, NG treated sample set to 1.

392 B) BMDMs were differentiated HG conditions. Cells were pretreated for 4 hours with NF-kappa
393 B inhibitor CAPE (5 μ M) and then treated with LPS at the concentration above for 16 hours.

394 RNA was isolated, cDNA was synthesized and *Acs11* mRNA copy number was determined by
395 qPCR. The data presented are means \pm standard errors of the means of three independent
396 experiments; the *P* value was calculated using one way ANOVA. Levels of significance: **p* <
397 0.05; ***p* < 0.01; and ****p* < 0.001.

398

399 **Figure 4. CHREBP and NF-kappa B increases ACSL1 transcriptional activity.** Expression
400 vectors of CHREBP, RELA (NFκB) or an empty vector were co-transfected with pACSL1-GLuc
401 reporter in HEK 293 cells cultured HG conditions. Luciferase assay was performed 48 hours
402 post transfection and shown as relative luciferase units (RLU). The data presented are means ±
403 standard errors of the means of three independent experiments; the P value was calculated
404 using one way ANOVA. Levels of significance: *p < 0.05; **p < 0.01; and ***p < 0.001.

405

406 **Figure 5. Model for glucose and inflammation induced *Acs1* expression by CHREBP and**
407 **NFκB in macrophages.** We propose that under A) normal glucose and low inflammation, there
408 is a small amount active CHREBP in the nucleus that promotes the expression of *Acs1*. B) In
409 high glucose this pool increases to promote a higher level of *Acs1* mRNA. C) During acute
410 inflammation, such as with treatment with LPS, NF-kappa B, which is normally held in check by
411 Inhibitor of kappa B (IκB), is free to translocate to the nucleus where it activates transcription of
412 *Acs1*, which can be accentuated by CHREBP.

413

414 **S1. Increased nuclear localization of CHREBP in macrophages in hyperglycemia.** A)
415 BMDMs were differentiated under NG and HG conditions. Cytoplasmic and membrane proteins
416 were isolated and western blot performed using an anti- CHREBP to determine the abundance
417 and subcellular localization of CHREBP protein. Tubulin and Histone H3 serve as controls for
418 cytoplasmic and nuclear fractions. B) BMDMs were differentiated under NG and HG conditions.
419 The cells were grown on cover slips and stained for CHREBP and DAPI to visualize the
420 nucleus. The images were obtained using Leica SP5 Confocal Microscope at 63X magnification.

421

422 **S2. Kinetics of ACSL1 induction by LPS treatment.** BMDMs were differentiated in NG and
423 treated with LPS (50ng/ml). RNA was isolated at the indicated times, cDNA was synthesized
424 and *Acs1* mRNA expression was determined by qPCR. The data presented are means ±

425 standard errors of the means of two independent experiments. Levels of significance: * $p < 0.05$;
426 ** $p < 0.01$; and *** $p < 0.001$.

427 **S3. ACSL1 protein abundance and membrane localized increase under inflammatory**

428 **conditions.** BMDMs were differentiated under NG conditions. A) Total cell lysates were
429 prepared after LPS treatment (50ng/ml for 24 hours) and ACSL1 protein abundance was
430 determined by western blot with an anti-ACSL1 antibody and with an anti-tubulin antibody as a
431 loading control. B) Bands were quantitated using the Image studio 5.2 and plotted using Graph
432 pad prism. The data presented are means \pm standard errors of the means of three independent
433 experiments. C) Cytoplasmic and membrane proteins were isolated to determine the
434 localization of ACSL1 protein by Western blotting upon LPS treatment. D) Image studio 5.2 was
435 used to quantify the bands and the values were plotted using Graph pad prism. The data
436 presented are means \pm standard errors of the means of three independent experiments.

437

438 **S4. LPS treatment increases CHREBP abundance in the nucleus.** BMDMs were
439 differentiated under NG and HG conditions. Cells were grown on cover slips, treated with LPS
440 (50ng/ml) for 24 hours and stained for CHREBP. The images were obtained using Leica SP5
441 Confocal Microscope at 63X magnification. Image J was used to quantify the fluorescence
442 intensity and Graph Pad Prism was used to plot the fluorescence intensities.

443

444 **S5. Predicted CHREBP and NF κ B sites upstream of ACSL1 promoter in the human and**
445 **mouse genes.** The Eukaryotic Promoter Database tool was used to predict the putative
446 CHREBP and NF κ B sites in human and mice upstream ACSL1 promoter region via the Jaspar
447 database. The P-value used in the prediction was $p < 0.01$.

448

449 **REFERENCES**

450

451 1. Moore KJ, Sheedy FJ, Fisher EA. Macrophages in atherosclerosis: a dynamic balance.
452 Nat Rev Immunol. 2013;13(10):709-21. Epub 2013/09/03. doi: 10.1038/nri3520. PubMed PMID:
453 23995626; PubMed Central PMCID: PMCPMC4357520.

454 2. Coleman RA. It takes a village: channeling fatty acid metabolism and triacylglycerol
455 formation via protein interactomes. J Lipid Res. 2019;60(3):490-7. Epub 2019/01/27. doi:
456 10.1194/jlr.S091843. PubMed PMID: 30683668; PubMed Central PMCID: PMCPMC6399496.

457 3. Kanter JE, Bornfeldt KE. Inflammation and diabetes-accelerated atherosclerosis: myeloid
458 cell mediators. Trends Endocrinol Metab. 2013;24(3):137-44. Epub 2012/11/17. doi:
459 10.1016/j.tem.2012.10.002. PubMed PMID: 23153419; PubMed Central PMCID:
460 PMCPMC3578033.

461 4. Kanter JE, Kramer F, Barnhart S, Averill MM, Vivekanandan-Giri A, Vickery T, et al.
462 Diabetes promotes an inflammatory macrophage phenotype and atherosclerosis through acyl-
463 CoA synthetase 1. Proc Natl Acad Sci U S A. 2012;109(12):E715-24. Epub 2012/02/07. doi:
464 10.1073/pnas.1111600109. PubMed PMID: 22308341; PubMed Central PMCID:
465 PMCPMC3311324.

466 5. Hu FB, Stampfer MJ, Haffner SM, Solomon CG, Willett WC, Manson JE. Elevated risk of
467 cardiovascular disease prior to clinical diagnosis of type 2 diabetes. Diabetes Care.
468 2002;25(7):1129-34. Epub 2002/06/28. doi: 10.2337/diacare.25.7.1129. PubMed PMID:
469 12087009.

470 6. Manichaikul A, Wang XQ, Zhao W, Wojczynski MK, Siebenthall K, Stamatoyannopoulos
471 JA, et al. Genetic association of long-chain acyl-CoA synthetase 1 variants with fasting glucose,
472 diabetes, and subclinical atherosclerosis. J Lipid Res. 2016;57(3):433-42. Epub 2015/12/30. doi:
473 10.1194/jlr.M064592. PubMed PMID: 26711138; PubMed Central PMCID: PMCPMC4766992.

474 7. Rubinow KB, Wall VZ, Nelson J, Mar D, Bomsztyk K, Askari B, et al. Acyl-CoA synthetase
475 1 is induced by Gram-negative bacteria and lipopolysaccharide and is required for phospholipid
476 turnover in stimulated macrophages. J Biol Chem. 2013;288(14):9957-70. Epub 2013/02/22. doi:
477 10.1074/jbc.M113.458372. PubMed PMID: 23426369; PubMed Central PMCID:
478 PMCPMC3617295.

479 8. Dreos R, Ambrosini G, Perier RC, Bucher P. The Eukaryotic Promoter Database:
480 expansion of EPDnew and new promoter analysis tools. Nucleic Acids Res. 2015;43(Database
481 issue):D92-6. Epub 2014/11/08. doi: 10.1093/nar/gku1111. PubMed PMID: 25378343; PubMed
482 Central PMCID: PMCPMC4383928.

483 9. Sanjabi S, Williams KJ, Sacconi S, Zhou L, Hoffmann A, Ghosh G, et al. A c-Rel
484 subdomain responsible for enhanced DNA-binding affinity and selective gene activation. Genes
485 Dev. 2005;19(18):2138-51. Epub 2005/09/17. doi: 10.1101/gad.1329805. PubMed PMID:
486 16166378; PubMed Central PMCID: PMCPMC1221885.

487 10. da Silva Xavier G, Rutter GA, Diraison F, Andreolas C, Leclerc I. ChREBP binding to fatty
488 acid synthase and L-type pyruvate kinase genes is stimulated by glucose in pancreatic beta-cells.
489 J Lipid Res. 2006;47(11):2482-91. Epub 2006/08/08. doi: 10.1194/jlr.M600289-JLR200. PubMed
490 PMID: 16891625.

491 11. Yang L, Yang Y, Si D, Shi K, Liu D, Meng H, et al. High expression of long chain acyl-
492 coenzyme A synthetase 1 in peripheral blood may be a molecular marker for assessing the risk
493 of acute myocardial infarction. Exp Ther Med. 2017;14(5):4065-72. Epub 2017/11/07. doi:
494 10.3892/etm.2017.5091. PubMed PMID: 29104625; PubMed Central PMCID:
495 PMCPMC5658692.

496 12. John S, Johnson TA, Sung MH, Biddie SC, Trump S, Koch-Paiz CA, et al. Kinetic
497 complexity of the global response to glucocorticoid receptor action. Endocrinology.
498 2009;150(4):1766-74. Epub 2009/01/10. doi: 10.1210/en.2008-0863. PubMed PMID: 19131569;
499 PubMed Central PMCID: PMCPMC2659280.

- 500 13. Abdul-Wahed A, Guilmeau S, Postic C. Sweet Sixteenth for ChREBP: Established Roles
501 and Future Goals. *Cell Metab.* 2017;26(2):324-41. Epub 2017/08/03. doi:
502 10.1016/j.cmet.2017.07.004. PubMed PMID: 28768172.
- 503 14. Uyeda K, Repa JJ. Carbohydrate response element binding protein, ChREBP, a
504 transcription factor coupling hepatic glucose utilization and lipid synthesis. *Cell Metab.*
505 2006;4(2):107-10. Epub 2006/08/08. doi: 10.1016/j.cmet.2006.06.008. PubMed PMID: 16890538.
- 506 15. Iizuka K, Bruick RK, Liang G, Horton JD, Uyeda K. Deficiency of carbohydrate response
507 element-binding protein (ChREBP) reduces lipogenesis as well as glycolysis. *Proc Natl Acad Sci*
508 *U S A.* 2004;101(19):7281-6. Epub 2004/05/01. doi: 10.1073/pnas.0401516101. PubMed PMID:
509 15118080; PubMed Central PMCID: PMCPMC409910.
- 510 16. Li MV, Chang B, Imamura M, Pongvarin N, Chan L. Glucose-dependent transcriptional
511 regulation by an evolutionarily conserved glucose-sensing module. *Diabetes.* 2006;55(5):1179-
512 89. Epub 2006/04/29. doi: 10.2337/db05-0822. PubMed PMID: 16644671.
- 513 17. Hurtado del Pozo C, Vesperinas-Garcia G, Rubio MA, Corripio-Sanchez R, Torres-Garcia
514 AJ, Obregon MJ, et al. ChREBP expression in the liver, adipose tissue and differentiated
515 preadipocytes in human obesity. *Biochim Biophys Acta.* 2011;1811(12):1194-200. Epub
516 2011/08/16. doi: 10.1016/j.bbali.2011.07.016. PubMed PMID: 21840420.
- 517 18. Pongvarin N, Chang B, Imamura M, Chen J, Moolsuwan K, Sae-Lee C, et al. Genome-
518 Wide Analysis of ChREBP Binding Sites on Male Mouse Liver and White Adipose Chromatin.
519 *Endocrinology.* 2015;156(6):1982-94. Epub 2015/03/10. doi: 10.1210/en.2014-1666. PubMed
520 PMID: 25751637; PubMed Central PMCID: PMCPMC4430618.
- 521 19. Al-Rashed F, Ahmad Z, Iskandar MA, Tuomilehto J, Al-Mulla F, Ahmad R. TNF-alpha
522 Induces a Pro-Inflammatory Phenotypic Shift in Monocytes through ACSL1: Relevance to
523 Metabolic Inflammation. *Cell Physiol Biochem.* 2019;52(3):397-407. Epub 2019/03/08. doi:
524 10.33594/000000028. PubMed PMID: 30845379.
- 525 20. Rhee SH, Hwang D. Murine TOLL-like receptor 4 confers lipopolysaccharide
526 responsiveness as determined by activation of NF kappa B and expression of the inducible
527 cyclooxygenase. *J Biol Chem.* 2000;275(44):34035-40. Epub 2000/08/23. doi:
528 10.1074/jbc.M007386200. PubMed PMID: 10952994.
- 529 21. Dorrington MG, Fraser IDC. NF-kappaB Signaling in Macrophages: Dynamics, Crosstalk,
530 and Signal Integration. *Front Immunol.* 2019;10:705. Epub 2019/04/27. doi:
531 10.3389/fimmu.2019.00705. PubMed PMID: 31024544; PubMed Central PMCID:
532 PMCPMC6465568.
- 533 22. Natarajan K, Singh S, Burke TR, Jr., Grunberger D, Aggarwal BB. Caffeic acid phenethyl
534 ester is a potent and specific inhibitor of activation of nuclear transcription factor NF-kappa B.
535 *Proc Natl Acad Sci U S A.* 1996;93(17):9090-5. Epub 1996/08/20. doi: 10.1073/pnas.93.17.9090.
536 PubMed PMID: 8799159; PubMed Central PMCID: PMCPMC38600.
- 537 23. Fornes O, Castro-Mondragon JA, Khan A, van der Lee R, Zhang X, Richmond PA, et al.
538 JASPAR 2020: update of the open-access database of transcription factor binding profiles.
539 *Nucleic Acids Res.* 2020;48(D1):D87-D92. Epub 2019/11/09. doi: 10.1093/nar/gkz1001. PubMed
540 PMID: 31701148; PubMed Central PMCID: PMCPMC7145627.
- 541 24. So AY, Cooper SB, Feldman BJ, Manuchehri M, Yamamoto KR. Conservation analysis
542 predicts in vivo occupancy of glucocorticoid receptor-binding sequences at glucocorticoid-induced
543 genes. *Proc Natl Acad Sci U S A.* 2008;105(15):5745-9. Epub 2008/04/15. doi:
544 10.1073/pnas.0801551105. PubMed PMID: 18408151; PubMed Central PMCID:
545 PMCPMC2311370.
- 546 25. Roelands J, Garand M, Hinchcliff E, Ma Y, Shah P, Toufiq M, et al. Long-Chain Acyl-CoA
547 Synthetase 1 Role in Sepsis and Immunity: Perspectives From a Parallel Review of Public
548 Transcriptome Datasets and of the Literature. *Front Immunol.* 2019;10:2410. Epub 2019/11/05.
549 doi: 10.3389/fimmu.2019.02410. PubMed PMID: 31681299; PubMed Central PMCID:
550 PMCPMC6813721.

Figure 1

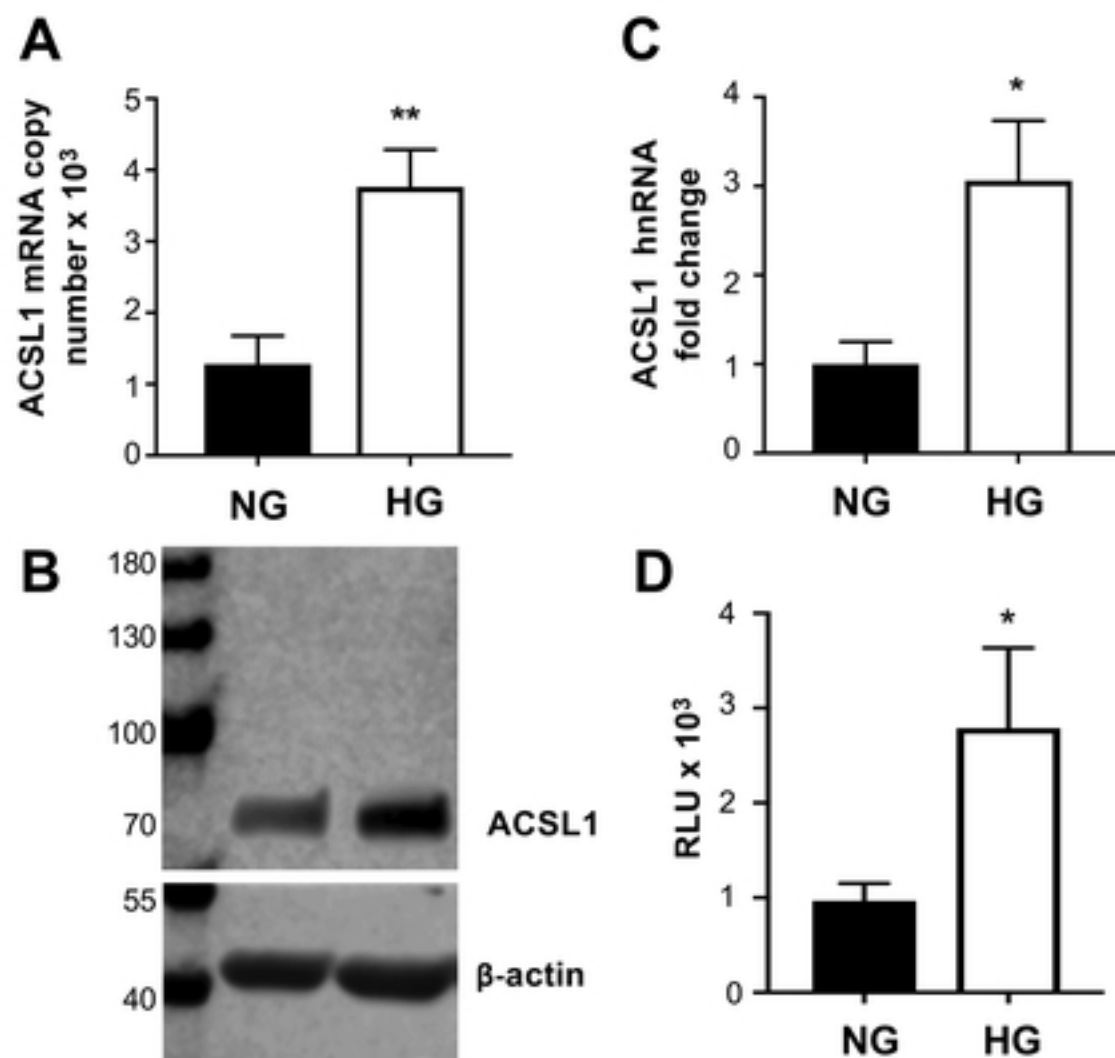


Figure 1

Figure 2

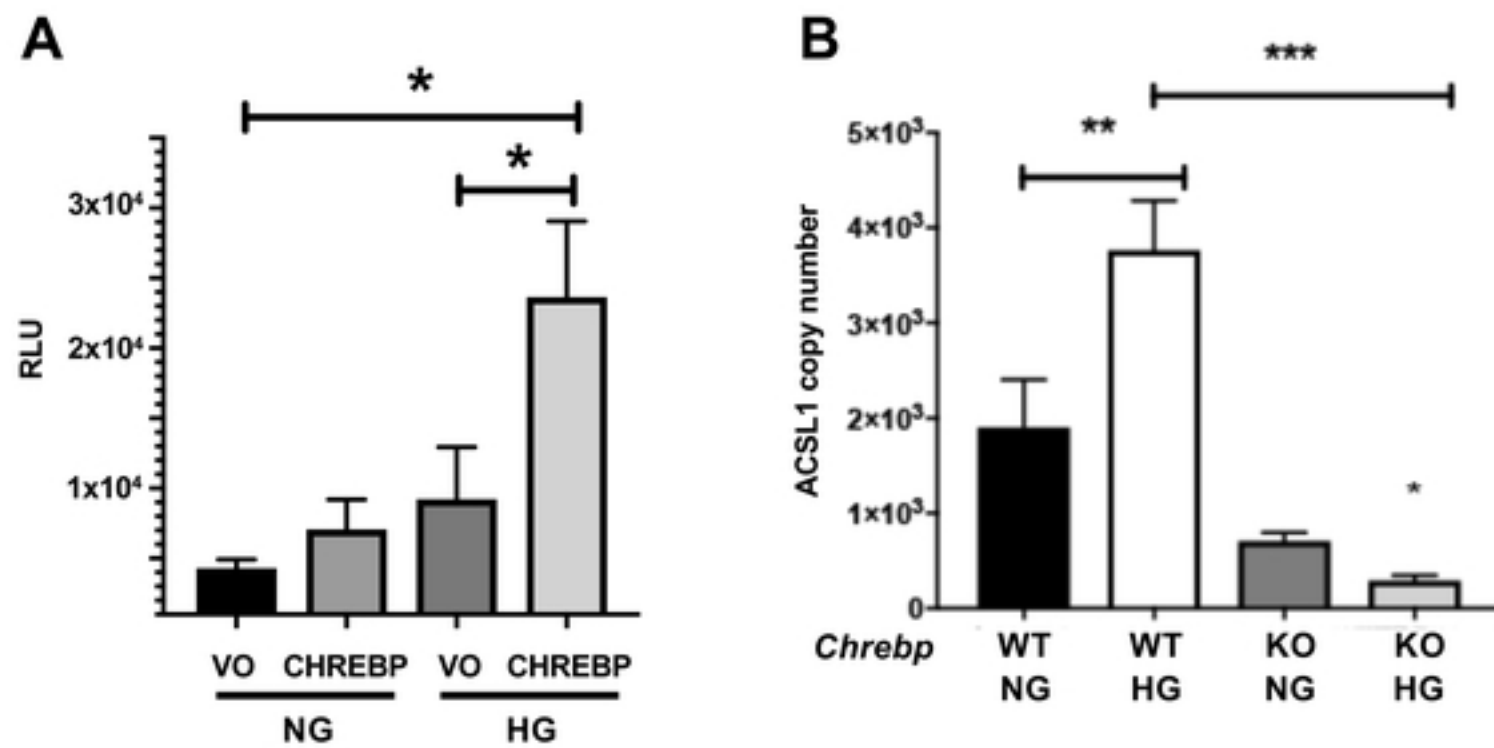


Figure 2

Figure 3

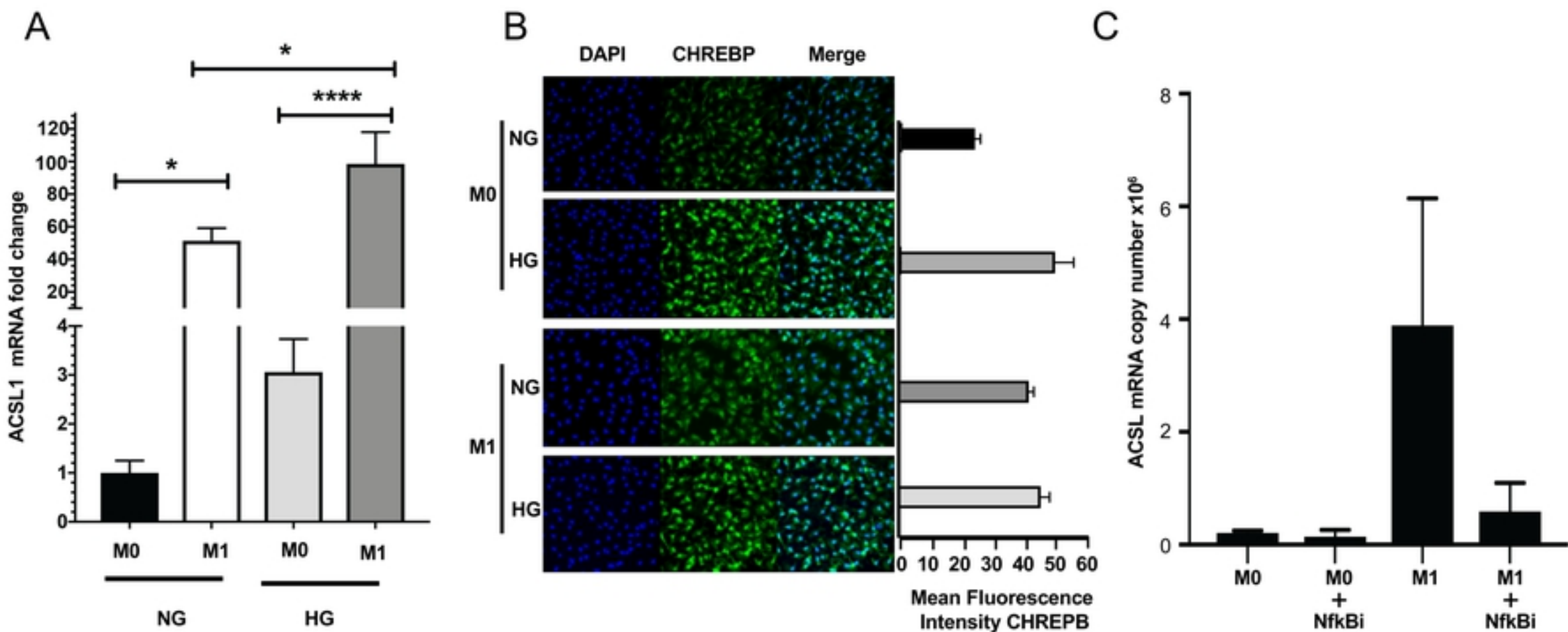


Figure 3

Figure 4

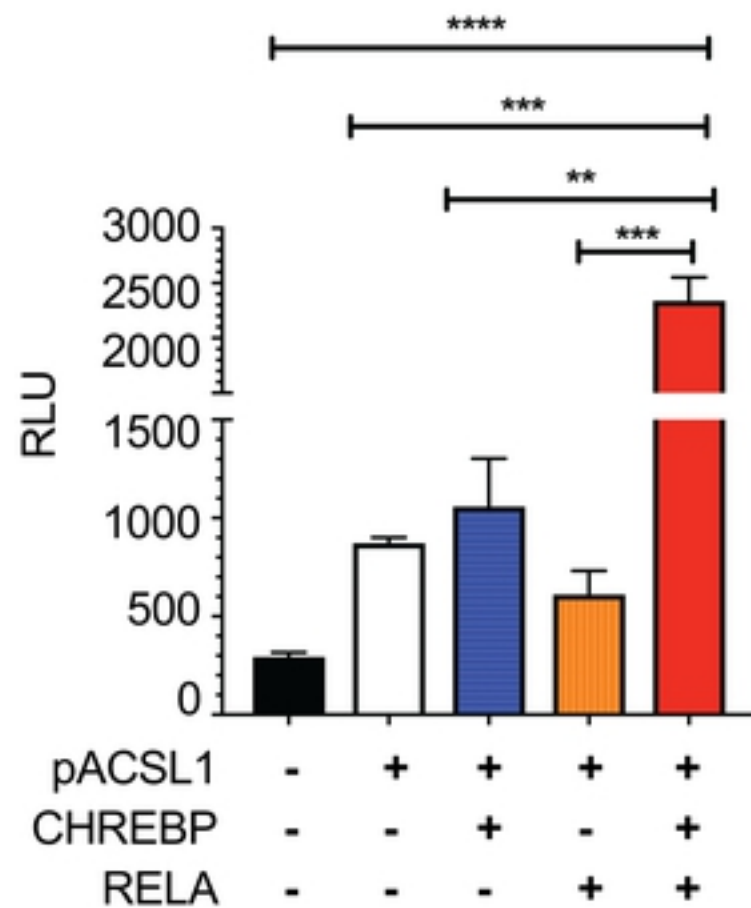


Figure 4

Figure 5

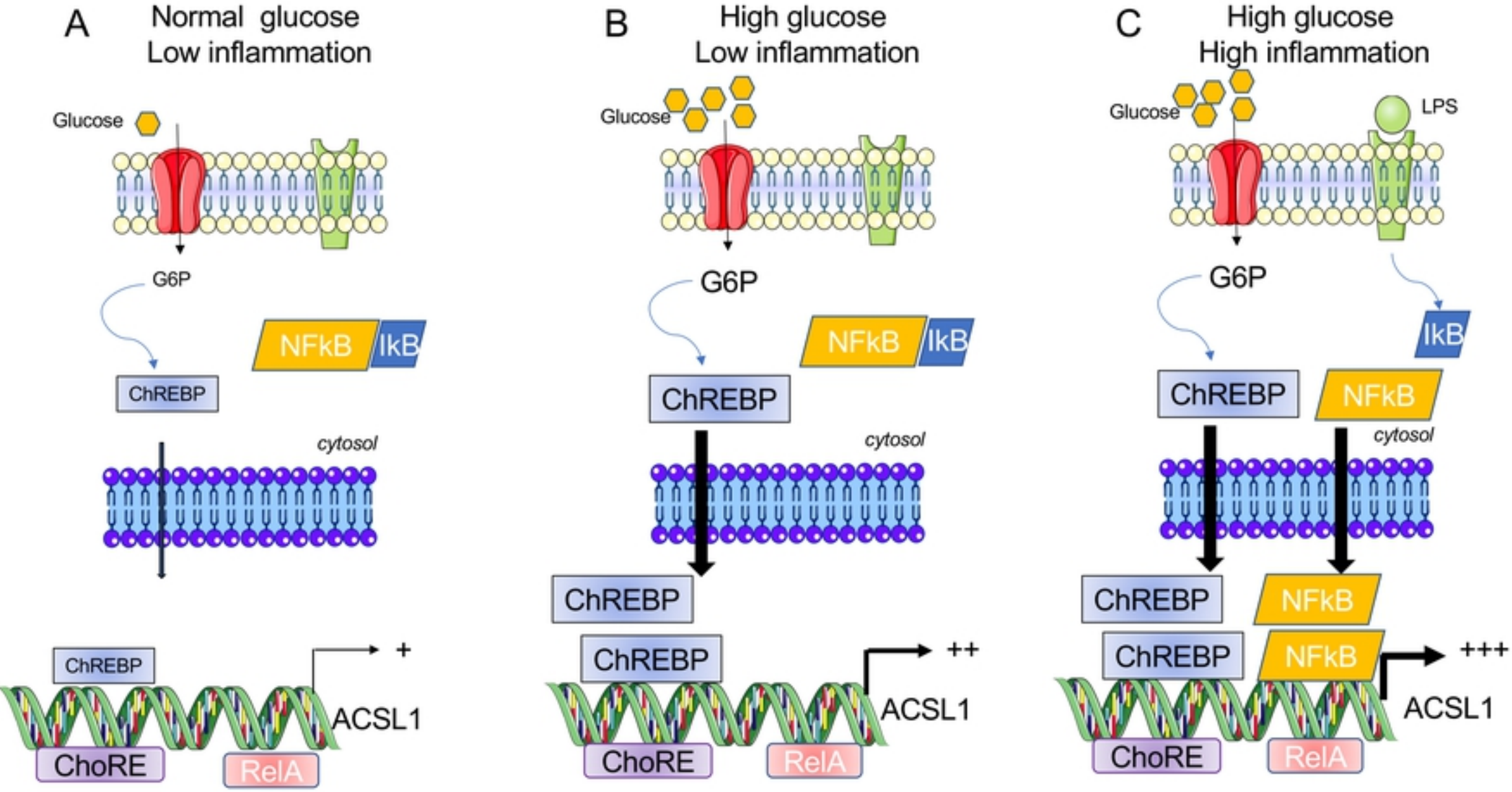


Figure 4